DOI 10.1007/s11595-016-1370-3

Kinetics and Mechanism of Adsorption of Phosphate on Fluorine-containing Calcium Silicate

ZHU Xinhua, ZHANG Zhao, SHEN Jun*

(College of Chemical Engineering, Sichuan University, Chengdu 610065, China)

Abstract: The nanowires-reticulated calcium silicate with a specific surface area more than 100 m^2/g was prepared by a hydrothermal process using hydrated lime ($Ca(OH)_2$, HL) and silica containing soluble fluoride, which was a by-product of fluorine industry, and the soluble fluoride in raw silica was fixed as $CaSiF_6$ at the same time. The kinetic characteristics and mechanism of adsorbing phosphate by fluorine-containing calcium silicate were investigated in the experiments of phosphorus (P) removal from aqueous solution. The results show that the prepared fluorine-containing calcium silicate has excellent performance for adsorbing phosphate, the adsorption process appears to follow pseudo-second-order reaction kinetics and the process is mainly controlled by chemisorption. The product resulted from P adsorption is mainly composed of hydroxyapatite (HAP) and fluorapatite (FAP), which are further used as adsorbents of heavy metal ion Cd^{2+} in aqueous solution and display excellent performance.

Key words: calcium silicate; P adsorption; Cd^{2+} adsorption; reaction kinetics; adsorption mechanism

1 Introduction

Calcium silicate is a new kind of eco-friendly material[1]. The extensive literatures indicate that calcium silicate has efficient removability for wastewater containing phosphate[2-4]. Calcium silicate adsorbs phosphorus (P) in the form of hydroxyapatite from aqueous solution through a simple and effective technology[5,6]. According to some studies, hydroxyapatite($Ca_{10}(PO_4)_6(OH)_2$, HAP) as a novel environmentally-functionalized material with special crystal structure[7,8] has showed excellent ion absorbability and exchangeability[9,10], which is characterized with high-efficiency adsorption capacity for most of heavy metal ions in wastewater, including Pb^{2+}, Cd^{2+}, Cu^{2+}, Zn^{2+}, Cr^{6+}, Mn^{2+}, Hg^{2+}, Fe^{3+}, Co^{2+}, and As^{3+}, *etc*[11-14]. In addition, the silica containing soluble fluoride of approximately 10 percent is a discharged waste from fluorine factory in large scale. At present, there are no effective management approaches and in most cases many factories pay not attention, so the released fluoride may cause severe ecological and environment issues[15]. It may be a better approach making the best of both aspects: the comprehensive use of fluorine-containing silica and treatment of the wastewater containing phosphate that the calcium silicate is synthesized using fluorine-containing silica from fluorine industry and hydrated lime (HL) as raw materials, and the synthesized fluorine-containing calcium silicate is used as an effective adsorbent for phosphate and heavy metal ions in wastewater.

The hydrothermal process conditions of fixing hazardous fluoride and preparing calcium silicate with high specific surface area using the by-product silica of fluorine industry and HL as raw materials were introduced in this study. The synthetic materials were used as the adsorbent of phosphate in aqueous solution. The adsorption kinetics and mechanism were investigated experimentally. The material obtained after adsorbing P was characterized and further used as the adsorbent for cadmium removal in aqueous solution, the performance of adsorbing Cd^{2+} of the material was evaluated.

2 Experimental

2.1 Preparation of calcium silicate

The siliceous material with the silica content of

(Received: Aug. 20, 2015; Accepted: Oct. 4, 2015)

ZHU Xinhua(朱新华俊): E-mail:zhuxinhua19@163.com

* Corresponding author: SHEN Jun(沈俊): Lecturer; Ph D; E-mail: junshen@aliyun.com

Funded by the Science and Technology-oriented Mid and Small-scale Enterprises Innovational Foundation of Ministry of Science and Technology of China(11C26216406395)

approximately 90% and the soluble fluoride content of approximately 10% was obtained from a fluorine industry and its specific surface area was only 8.1 m^2/g. Calcareous material ($Ca(OH)_2$, HL, AR.) was purchased from Chengdu Kelong Chemical Co. Ltd.

The silica and HL were mixed together with the Ca/Si (calcium /silicon molar ratio) of 0.7, then the mixtures were agitated by a ultrasonic generator for 5 min, the suspensions of 58.6 mL with a liquid/solid ratio of 10 were obtained, the suspensions were transferred to a hydrothermal reactor heated at 120, 140, and 160℃ for 8 h, respectively, and taken out when the temperature of reaction systems was reduced to room temperature. The obtained products were dried at 120 ℃ for 10 h and used as adsorbents in the following adsorption experiments. Three samples from 120, 140, and 160 ℃, were indexed as A, B, and C, respectively.

2.2 P adsorption test

The 1 000 mL simulated solutions with initial P concentration of 100 mg/L or 56.12 mg/g were prepared by adding KH_2PO_4 (AR). The prepared calcium silicate of 1.0 g was placed into a beaker with the P simulation solution located in a water bath and shaken at a constant rate of 100 r/min under controlled temperature condition (25 ℃) to keep the powder sample in complete suspension. During adsorption, the sample of 25 mL was taken from the suspension at various intervals, filtered and pipetted into 150 mL erlenmeyer flask for determination of the P concentration until the P concentration of solution sample no longer changed. After adsorption experiments, the suspensions were filtered, the sediments were obtained and dried at 120 ℃ for 10 h. Then the P contents of sediments could be calculated as Eq.(1):

$$q_{\mathrm{P}} = \frac{(c_0 - c_{\mathrm{t}}) \times v}{\omega} \times 100\% \qquad (1)$$

where, q_{p} is the amount of phosphorus adsorbed by per unit mass adsorbent (mg/g), c_{t} is the restrained P concentration in solution (mg/L), c_0 is the initial P concentration (mg/L), ω is the mass of adsorbent (mg) and v is the volume of the simulation solution (L).

2.3 Cd^{2+} adsorption test

The metal cadmium powder (purity of 99.99%) was dissolved in HNO_3 solution (1+1, in volume), after heating and boiling, a simulated cadmium standard solution was obtained. The pH value of the solution was adjusted to neutral with HNO_3 solution of 6 mol/L and NaOH solution of 6 mol/L prior to adsorption experiments. The sediment samples of 0.5 g from P adsorption test were placed into a beaker with simulated cadmium solution located in the water bath and shaken at a constant rate of 100 r/min under controlled temperature condition (25 ℃) to keep the powder sample in complete suspension. The solution samples of 25 mL were taken from the suspension at various intervals, and pipetted into 250 mL separating funnel after filtration, and the residual concentration of Cd^{2+} was detected by dithizone spectrophotometric method (GB 7471-87) with a ultraviolet spectrophotometer (TU-1810). The method's lowest detectable concentration for Cd^{2+} was 0.001 mg/L and the linear equation of standard curve (Y=0.9541X−0.013, the correlation coefficient of 0.9970) was obtained in the experiment.

The cadmium contents q_{Cd} of adsorbent samples after cadmium adsorption, which is the capacity of adsorbent, could be calculated using Eq.(2):

$$q_{\mathrm{Cd}} = \frac{(c_0 - c_{\mathrm{t}}) \times V}{m} \times 100\% \qquad (2)$$

where, c_{t} is the restrained cadmium concentration in the simulation solution (mg/L), c_0 is the initial cadmium concentration (mg/L), m is the mass of adsorbent (mg) and V is the volume of the simulation solution (L).

2.4 Characterization methods of solid sample

X-ray diffraction (XRD) patterns of samples were recorded with an X-ray diffractometer (D/Max-rA, Japan) using Cu Kα radiation. SEM images were collected on an S-4800 scanning electron microscope (Hitachi, Japan). Brunauer-Emmett-Teller (BET) surface areas were measured from N_2 adsorption isotherms by homemade adsorption instrument according to Chinese national standard (GB/T 19587-2004 Determination of the specific surface area of solids by gas adsorption using the BET method).

3 Results and discussion

3.1 Preparation and characteristics of calcium silicate

As adsorption material, the high specific surface area not only provides more adsorption and ion exchange sites, but also can enhance the adsorbability of the material[16]. The experiments show that the specific surface area of the prepared calcium silicate is affected by Ca/Si molar ratio, hydrothermal temperature and reaction time. Further experiments discovered that shorter reaction time is not helpful for complete

conversion of raw materials, and higher reaction time requires more energy. So the proper reaction time of 8 h was determined in the experiment. The relationship between the specific surface area and the experiment condition (Ca/Si molar ration and hydrothermal temperature) of material preparation is shown in Table 1 and Table 2. From the above tables it can be seen that the Ca/Si molar ratio has the most significant impact on the specific surface area of samples in a certain reaction time and secondarily hydrothermal temperature, and the optimal conditions are Ca/Si molar ratio of 0.7, hydrothermal temperature maintained from 120 ℃ to 140 ℃ and reaction time of 8 h.

Table 1 Specific surface area of the samples prepared by 140 ℃

Ca/Si	0.4	0.5	0.6	0.7	0.8	0.9
Specific surface area/($m^2 \cdot g^{-1}$)	45.49	90.32	102.13	122.49	112.20	70.21

Table 2 Specific surface area of the samples prepared at Ca/Si=0.7

Temperature/℃	120	140	160
Specific surface area /($m^2 \cdot g^{-1}$)	143.82	122.49	106.44

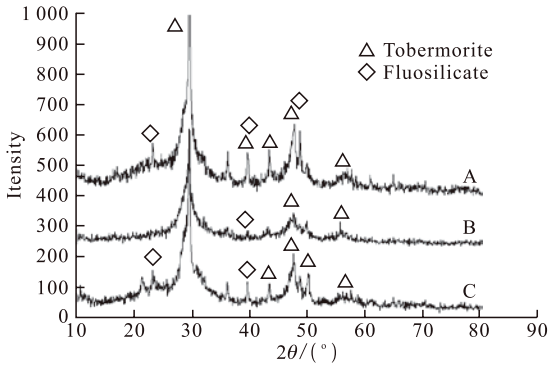

Fig.1 XRD patterns of samples prepared at different temperatures: (a) 120 ℃; (b) 140 ℃ and (c)160 ℃

The composition of the prepared samples A, B, and C is mainly tobermorite (PDF card 29-0329, $Ca_5Si_6O_{16}(OH)_2$), which is simply named as calcium silicate subsequently, and calcium fluosilicate (PDF card 01-0482, $CaSiF_6$) based on transformation of the soluble fluoride in the raw material (Fig.1). The free fluorine content is up to 99.52 mg/g in initial raw materials, but during the hydrothermal reaction preparing calcium silicate, the fluorine releasing into the solution is only around 0.3 mg/g because of the formed $CaSiF_6$ with very small solubility. Three samples: A, B, and C have high specific surface area of 143.8, 122.5, and 106.4 m^2/g because they have a developed space connected mesh structure (Fig.2), which is of benefit to strengthen the adsorption mass transfer process and shorten the adsorption equilibrium time.

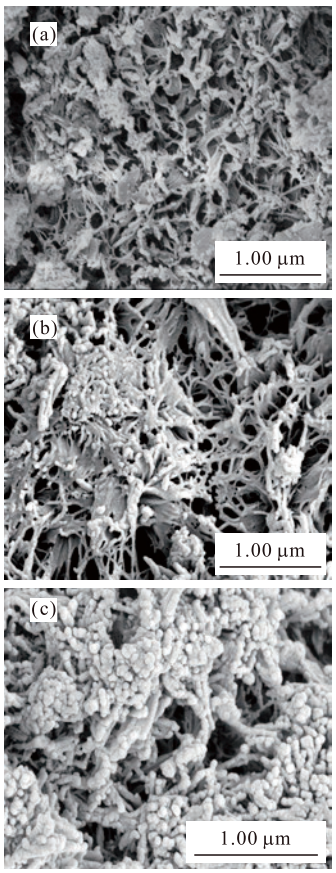

Fig.2 SEM images of the prepared calcium silicate: (a) A120 ℃, (b)B140 ℃ and (c) C160 ℃

3.2 Kinetic equation of P adsorption

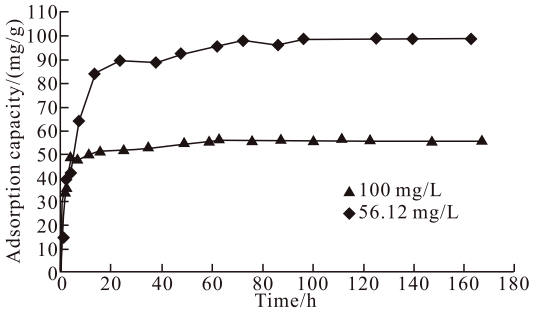

Fig.3 Adsorption performance of calcium silicate in different initial P concentrations

The pH value of P adsorption system runs from 7.5 to 8.5 (the pH of the system itself), which promotes adsorbing P and forming apatite of calcium silicate from wastewater[1,17]. Under the same adsorption conditions, the P adsorption characteristics of the prepared calcium silicate sample B for different initial P concentrations (56.12 mg/L and 100 mg/L)

in aqueous solution are shown in Fig.3. It can be seen that the adsorption rate at different P concentrations decreases rapidly after the first 4 h, then the adsorption capacities keep unchanged. Moreover, the lower initial P concentration accelerates adsorption rate and shortens adsorption equilibrium time, and the adsorption process carries out thoroughly. By contrast, the higher initial P concentration is favorable to increase P adsorption capacity.

In spite of many mathematical models proposed to interpret the transport of solutes inside adsorbent, the complexity of mathematical models makes them inconvenient in practice[18]. The pseudo-first-order (Eq.3)) and pseudo-second-order (Eq.(4)) kinetic models are applied to study the adsorption dynamics of solid sorbent because of their good applicability in many cases[19]:

The pseudo-first-order equation:

$$\ln(q_e - q_t) = \ln q_e - k_1 t \tag{3}$$

The pseudo-second-order equation:

$$\frac{t}{q_t} = \frac{1}{k_2 q_e^2} + \frac{t}{q_e} \tag{4}$$

where, q_e(mg/g) is the amount of equilibrated adsorption capacity, q_t(mg/g) is the amount of P adsorption capacity at the time t (min), and k_1(min^{-1}) and k_2(g·mg^{-1}·min^{-1}) are the constants of the pseudo-first-order and pseudo-second-order equation, respectively. The dynamic models are applied to fit experimental data and the results are shown in Fig.4 and Fig.5, and the kinetic parameters are shown in Table 3.

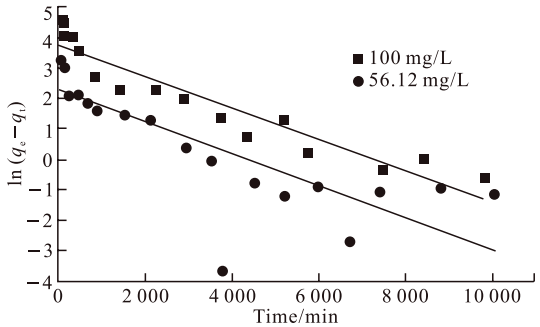

Fig.4 Linearized pseudo-first-order kinetic plots for P adsorption in different initial concentrations

From Fig.4 and Table 3, the pseudo-first-order kinetics model shows poor fitting for the low concentration solution with the linear correlation coefficient of 0.6389 and a margin of error of 82% between theoretical and experimental values. However, as shown in Fig.5 and Table 3, the pseudo-second-order kinetics model provides preferable match between theoretical and experimental values, and the pseudo-second-order kinetics model has a better correlation for experimental data than the pseudo-first-order kinetics model. Besides, for the high concentration solution, the experimental data more conform to pseudo-second-order equation. As a result, the adsorption process appears to follow pseudo-second-order reaction kinetics, which suggests that the process is mainly controlled by chemisorption[20,21]. Moreover, the correlation of pseudo-first-order equation increases with increasing initial P concentration, which suggests that the high concentration solution strengthens the driving force of adsorption by a concentration difference of the external mass transfer[22,23], and the P adsorption process is the result of external mass transfer and chemisorption.

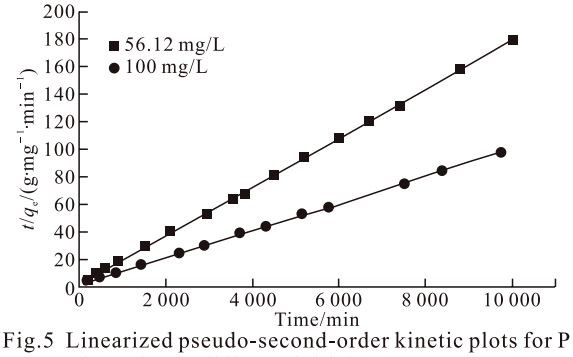

Fig.5 Linearized pseudo-second-order kinetic plots for P adsorption in different initial concentrations

The total P adsorption capacity, residual P concentration and the exchange rate of Ca^{2+} are used to explore the influence of initial concentration on P adsorption. As shown in Table 4, the adsorption performance of calcium silicate samples A, B, and C changes with change of the initial P concentration, the effective P removability for the simulation solution with a low concentration P is more than 99.8%, and residual P concentration is less than 0.1 mg/L, which has attained the level 1 standard of comprehensive

Table 3 Kinetic parameters for P adsorption by calcium silicate under different initial concentration

Concentration/(mg/L)	Pseudo-first-order kinetic			Pseudo-second-order kinetic			Measured
	q_e	k_1	R_1^2	q_e	k_2	R_2^2	q_e
56.12	10.030 2	0.000 5	0.638 9	56.179 8	2.83×10^{-4}	0.999 9	55.740 5
100	44.119 4	0.000 5	0.907 8	102.040 8	4.50×10^{-5}	0.999 4	99.501 2

Table 4 Effect of initial P concentration on adsorption performance of calcium silicate

P concentration/(mg·L^{-1})	Performance	A(120 ℃)	B(140 ℃)	C(160 ℃)
56.12	Residual P concentration	0.1325	0.066 0	0.095 4
	P removal rate	99.76%	99.88%	99.83%
100	Residual P concentration	0.1545	0.1288	0.2246
	P removal rate	99.72%	99.87%	99.60%

discharge standard of sewage of China (GB 8978-1996).

3.3 Mechanism of P adsorption

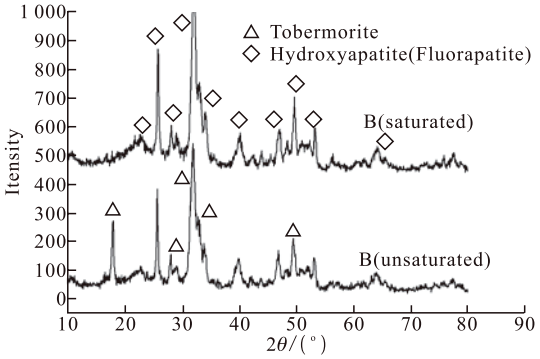

Fig.6 X-ray diffraction patterns of samples after P adsorption

The XRD patterns of the samples applied in adsorbing P test are shown in Fig.6. There the diffraction peaks of tobermorite (calcium silicate) are discovered when sample B was used in adsorbing P but unsaturated. However, the diffraction peaks of tobermorite and fluosilicate no longer appear, and the principal peaks of apatite (PDF card 09-0432, HAP; PDF card 03-0747, FAP) emerge at 25.88°, 31.76°, and 53.26° for the saturated sample B, which indicates that P adsorption process is realized by converting calcium silicate and calcium fluosilicate into apatite on the surface. Some researches suggest that the XRD peaks of HAP and FAP are similar and the phase is apatite, additionally, the crystallinity of FAP increases with the sharper correlation peaks related to HAP, and the stability of apatite is increased by adding fluorine[24-26].

In the phosphorus removal process of fluorine-containing calcium silicate, the fluorine was transferred to apatite and existed in the form of FAP. FAP widely exists in nature, the enamel surface of teeth was FAP, with excellent stable property and no releasing fluorine to worry about. So the new formed fluorine compound after P adsorption will not cause secondary pollution.

Table 5 Elemental composition of samples before and after P adsorption

Element	Before adsorption		After adsorption	
	Weight/%	Atomic/%	Weight/%	Atomic/%
Oxygen	45.62	62.04	46.18	63.94
Fluorine	4.81	5.51	3.16	3.69
Silicon	23.88	18.50	9.56	7.54
Phosphorus	–	–	13.02	9.31
Calcium	25.7	13.95	28.08	15.52

EDS analysis results of sample B, before and after adsorption process, are presented in Fig.7, indicating that phosphorus emerges after adsorption. The data in Table 5 reveal that the Ca/P molar ratio of sample B after adsorption is near 5:3 in similar proportion on HAP and FAP, which further proves adsorption process realized by converting calcium silicate to apatite on the surface.

SEM images of sample B before and after adsorption are shown in Fig.8. From Fig.8, there are obvious changes in the morphology of adsorbent after adsorption, from initial nanowires-reticulation (before adsorption, Fig.8(a)) to needle (after adsorption of a period of time, Fig.8(b)), then to disintegrated short bar structure (after adsorption saturation, Fig.8(c)).

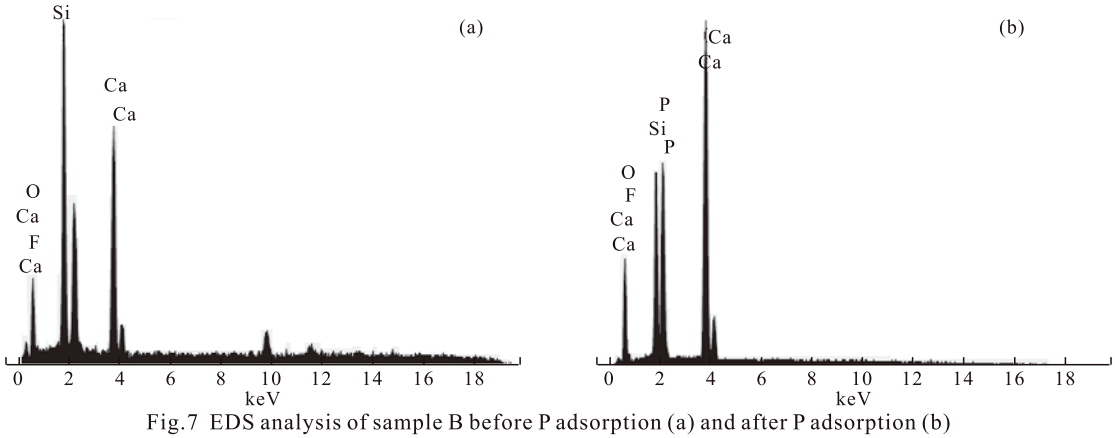

Fig.7 EDS analysis of sample B before P adsorption (a) and after P adsorption (b)

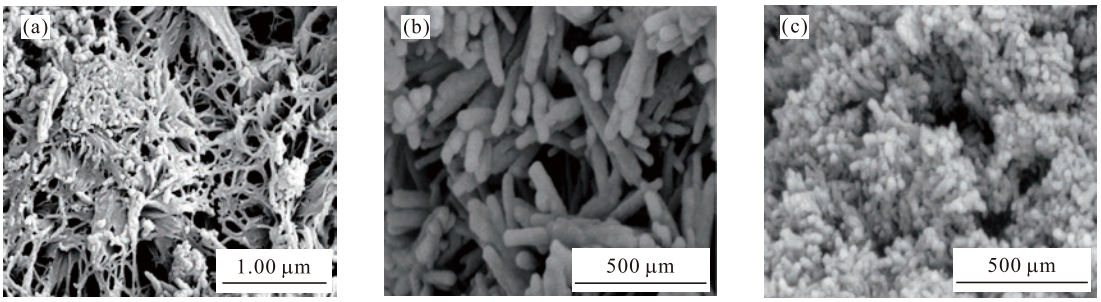

Fig.8 SEM images of samples: (a) before P adsorption and (b) P adsorption after a period of time and (c) after P adsorption saturation

In general, P adsorption principle of calcium silicate is described based on crystallization process, in which calcium silicate used as the crystal seed promotes combining the phosphate ion with calcium ion in solution to crystallize out apatite crystal within a certain range of pH[27-29]. In our experiments, however, these changes are based on not only complete transition of phase (Fig.6), but also distinct morphology (Fig.8), which is not corresponding to the principle of a simple crystallization.

In conclusion, the mechanism of adsorbtion of phosphate on fluorine-containing calcium silicate can be described as the following three processes: dissolution of Ca^{2+}, the formation of nucleus of apatite with the disintegrable space structure, and growth of apatite micro-crystal with a large number of separating crystalline grains. In the practical adsorption process, these are not independent and are reaction simultaneously to form a new phase, apatite. Because Ca^{2+} ions are homogeneously inlaid in the pore structure and dissolve slowly, the adsorption equilibrium time will be longer than that of a crystallization process, agreeing with the long saturated adsorption time in our experiments. Therefore, the dissolution of Ca^{2+} is the rate determining step of P adsorption process.

The specific surface area of sample B after adsorption remains as high as 128.4 m^2/g, which can further provide a probability as adsorbent for heavy metal ions in solution.

3.4 Cd^{2+} adsorption

From Table 5 and Fig.6, it is evident that the major components of surface of sample B after P adsorption are HAP and FAP. The soluble fluoride in raw silica further transforms into more stable apatite crystal during the process of P adsorption. Generally, the mechanism of the metal cation exchange of HAP includes: ion exchange, adsorption, dissolution/precipitation, and formation of surface complexes[30-32]. Moreover, the crystal structure and the ionic radius similarity of HAP determine that the Ca^{2+} in lattice can be exchanged by certain cations (Pb^{2+}, Cd^{2+}, Zn^{2+}, and Hg^{2+}, *etc*), and the OH^- in lattice can be exchanged by certain anions (F^-, HCO_3^-, *etc*). Because the structure of FAP is similar to HAP and more stability, it is considered that FAP has the similar adsorption mechanism corresponding to HAP and removal capacity for heavy metal ions.

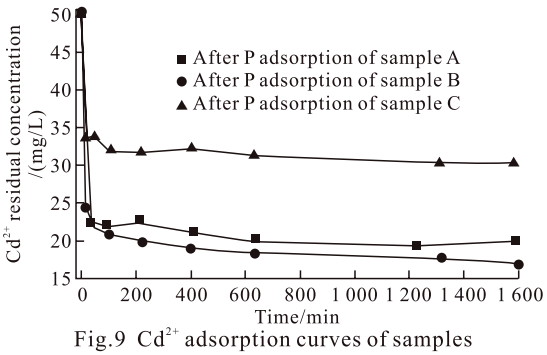

Fig.9 Cd^{2+} adsorption curves of samples

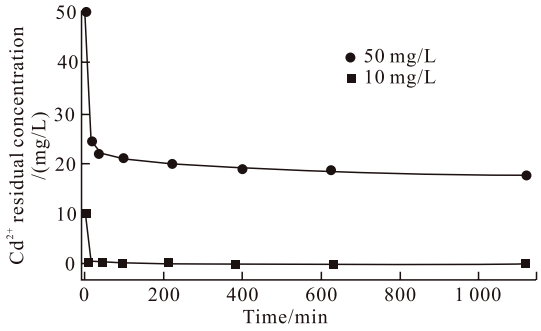

Fig.10 Effect of initial Cd^{2+} concentration on adsorption performance

For the simulation solution with the Cd^{2+} concentration of 50 mg/L, the adsorption tests of Cd^{2+} of samples A, B, and C after P adsorption are shown in Fig.9. It can be seen that the concentration of Cd^{2+} decreases sharply for 0-30 min and adsorption reaches equilibrium in 80 min. Furthermore, there is significant relation between the preparation temperature and the adsorptive performance of samples. The samples A and B display excellent behavior, the maximal Cd^{2+} adsorption capacity of the prepared sample is 67.4 mg/g, which indicates that the specific surface area of

material as adsorbent is closely related to the maximal Cd^{2+} adsorption capacity and Cd^{2+} removability.

The relationship between Cd^{2+} removability and initial Cd^{2+} concentration of adsorption system is shown in Fig.10, which indicates that the removal rate decreases with increasing concentration of Cd^{2+}. Moreover, when the initial concentration is below 10 mg/L, the removal rate of Cd^{2+} is close to 100%, and the residual Cd^{2+} concentration in solution can reach the comprehensive discharge standards of sewage (GB 8978-1996) and the drinking-water standards of China.

4 Conclusions

The nanowires-reticulated calcium silicate ($Ca_5Si_6O_{16}(OH)_2$) with a specific surface area more than 100 m^2/g can be prepared by a hydrothermal process using hydrated lime ($Ca(OH)_2$) and silica containing soluble fluoride, and 99.7% of the soluble fluorine was fixed as calcium fluosilicate ($CaSiF_6$). The fluorine-containing calcium silicate materials display excellent performances for removing phosphate from aqueous solution. The P removal rate is as high as 99%. The process appears to follow pseudo-second-order reaction kinetics and is mainly controlled by chemisorption. The fluorine-containing calcium silicate is transformed to hydroxyapatite (HAP) and fluorapatite (FAP) after adsorbing phosphate and still keeps a high specific surface area, which is propitious to adsorb some heavy metal ions from aqueous solution. The maximal Cd^{2+} adsorption capacity of the prepared sample is 67.4 mg/g and Cd^{2+} removal rate can approach 100% when the simulation solution with initial concentration of Cd^{2+} 10 mg/L is treated, which meets the drinking-water standards of China.

References

[1] Okano K, Uemoto M, Kagami J, *et al.* Novel Technique for Phosphorus Recovery from Aqueous Solutions Using Amorphous Calcium Silicate Hydrates(A-CSHs)[J]. *Water Research*, 2013, 47(7):2251-2259

[2] Renman A, Renman G. Long-term Phosphate Removal by the Calcium-silicate Material Polonite in Wastewater Filtration Systems[J]. *Chemosphere*, 2010, 79(6): 659-664

[3] Sengupta S, Pandit A. Selective Removal of Phosphorus from Wastewater Combined with Its Recovery as a Solid-phase Fertilizer[J]. *Water Research*, 2011, 45(11): 3 318-3 330

[4] Liu Y, Sheng X, Dong YH, *et al.* Removal of High-concentration Phosphate by Calcite: Effect of Sulfate and pH[J]. *Desalination*, 2012, 289(15): 66-71

[5] Chen XC, Kong HN, Wu DY, *et al*. Phosphate Removal and Recovery Through Crystallization of Hydroxyapatite Using Xonotlite as Seed Crystal[J]. *Journal of Environmental Sciences*, 2009, 21(5): 575-580

[6] Song YH, Peter GW, Berg U, *et al*. Calcite-seed Crystallization of Calcium Phosphate for Phosphorus Recovery[J]. *Chemosphere*, 2006, 63(2): 236-243

[7] Simon FG, Biermann V, Peplinski B, *et al.* Uranium Removal from Groundwater Using Hydroxyapatite[J]. *Applied Geochemistry*, 2008, 23(8): 2 137-2 145

[8] Sundaram CS, Viswanathan N, Meenakshi S, *et al.* Defluoridation Chemistry of Synthetic Hydroxyapatite at Nano Scale: Equilibrium and Kinetic Studies[J]. *Journal of Hazardous Materials*, 2008, 155 (1-2): 206-215

[9] Krestou A, Xenidis A, Panias D. Mechanism of Aqueous Uranium (VI) Uptake by Hydroxyapatite[J]. *Minerals Engineering*, 2004, 17(3): 373-381

[10] Feng Y, Gong JL, Zeng GM, *et al.* Adsorption of Cd(II) and Zn(II) from Aqueous Solutions Using Magnetic Hydroxyapatite Nanoparticles as Adsorbents[J]. *Chemical Engineering Journal*, 2010, 162(2): 487-494

[11] Gòmez del Río J, Sanchez P, Morando PJ, *et al.* Retention of Cd, Zn and Co on Hydroxyapatite Filters[J]. *Chemosphere*, 2006, 64(6): 1 015-1 020

[12] Corami A, Mignardi S, Ferrini V. Copper and Zinc Decontamination from Single and Binary-metal Solutions Using Hydroxyapatite[J]. *Journal of Hazardos Materials*, 2007, 146(1-2): 164-170

[13] Czerniczyniec M, Farias S, Magallanes J, *et al.* Arsenic Adsorption on Biogenic HAP: Solution Compositon Effects[C]. In: *11th International Conference on Surface and Colloid Science*. Foz do Iguazu, Brazil, 2003, 269

[14] Fuller C, Bargar J, Davirs J, *et al.* Mechanisms of Uranium Interactions with Hydroxyapatite: Implications for Ground Water Remediation[J]. *Environmental Science and Technology*, 2002, 36:158-165

[15] Jiménez-Reyes M, Solache-Ríos M. Sorption Behavior of Fluoride Ions from Aqueous Solutions by Hydroxyapatite[J]. *Journal of Hazardous Materials*, 2010, 180(1-3): 297-302

[16] Zhu XH, Zhang Z, Shen J. Preparation of Calcium Silicate Using Hazardous Solid Wastes and Its Application in Treatment of Phosphate-containing Wastewater[C]. In: *2014 International Conference on Material Science and Environmental Engineering. Switzerland: Trans Tech Publications*, 2014:652-658

[17] Battistoni P, De Angelis A, Pavan P, *et al*. Phosphorus Removal from a Real Anaerobic Supernatant by Struvite Crystallization[J]. *Water Research*, 2001, 35(9): 2 167-2 178

[18] Biswas BK. Inoue K, Ghimire KN, *et al.* The Adsorption of Phosphate from an Aquatic Environment Using Metal-loaded Orange Waste[J]. *Journal of Colloid and Interface Science*, 2007, 312(2): 214-223

[19] Özacar M. Equilibrium and Kinetic Modeling of Adsorption of Phosphorus on Calcined Alunite [J]. *Adsorption*, 2003, 9(2); 125-132

[20] Uzun I, Güzel F. Rate Studies on the Adsorption of Some Dyestuffs and p-nitrophenol by Chitosan and Monocarboxymethylated(mcm)-chitosan from Aqueous Solution[J]. *Journal of Hazardous Materials*, 2005, B118(1-3): 141-154

[21] Chiou MS, Li HY. Adsorption Behavior of Reactive dye in Aqueous Solution on Chemical Cross-linked Chitosan Beads[J]. *Chemosphere*, 2003, 50(8): 1 095-1 105

[22] Annadurai G, Ling LY, Lee JF. Adsorption of Reactive Dye from an Aqueous Solution by Chitosan: Isotherm, Kinetic and Thermodynamic Analysis[J]. *Journal of Hazardous Materials*, 2008, 152(1): 337-346

[23] Skodras G, Diamantopoulou I, Pantoleontos G, *et al.* Kinetic Studies of Elemental Mercury Adsorption in Activated Carbon Fixed Bed Reactor[J]. *Journal of Hazardous Materials*, 2008, 158(1):1-13

[24] Smahi A, Solhy A, Badaoui HE, *et al.* Potassium Fluoride Doped Fluorapatite and Hydroxyapatite as New Catalysts in Organic Synthesis[J]. *Applied Catalysis A: General*, 2003, 250(1):151-159

[25] Tredwin CJ, Georgiou G, Kim HW, *et al.* Hydroxyapatite, Fluor-Hydroxyapatite and Fluorapatite Produced via the Sol-gel Method: Bonding to Titanium and Scanning Electron Microscopy[J]. *Dental Materials*, 2013, 29(5): 521-529

[26] Gross KA, Bhadng KA. Sintered Hydroxyfluorapatites. Part III: Sintering and Resultant Mechanical Properties of Sintered Blends of Hydroxyapatite and Fluorapatite[J]. *Biomaterials*, 2004, 25(7-8):1 395-1 405

[27] Chen XC, Kong HN, Wu DUY, *et al.* Phosphate Removal and Recovery Through Crystallization of Hydroxyapatite Using Xonotlite as Seed Crystal[J]. *Journal of Environment Sciences*, 2009, 21(5): 575-580

[28] Berg U, Donnert D, Ehbrecht A, *et al.* "Active Filtration" for the Elimination and Recovery of Phosphorus from Waste Water[J]. *Colloids and Surfaces A: Physicochemical and Engineering*, 2005, 265(1-3):141-148

[29] Jang H, Kang SH. Phosphorus Removal Using Cow Bone in Hydroxy-apatite Crystallization[J]. *Water Research*, 2002, 36(5): 1 324-1 330

[30] Srinivasan M, Ferraris C, White T. Cadmium and Lead Ion Capture with Three Dimensionally Ordered Macroporous Hydroxyapatite[J]. *Environmental Science & Technology*, 2006, 40: 7 054-7 059

[31] Xu YP, Schwartz FW, Traina SJ. Sorption of Zn^{2+} and Cd^{2+} on hydroxyapatite Surfaces[J]. *Environmental Science and Technology*, 1994, 28: 1 472-1 480

[32] Mobasherpour I, Salahi E, Pazouki M. Comparative of the Removal of Pb^{2+}, Cd^{2+} and Ni^{2+} by Nano Crystallite Hydroxyapatite from Aqueous Solutions: Adsorption Isotherm Study[J]. *Arabian Journal of Chemistry*, 2012, 5(4): 439-446